

Superconductivity near the mobility edge

D. Shahar* and Z. Ovadyahu

Racah Institute of Physics, The Hebrew University, Jerusalem, Israel 91904

(Received 30 April 1992)

We study the low-temperature transport properties of amorphous indium oxide films as a function of disorder near the metal-insulator transition. Deep in the insulating regime, the conductivity shows simple variable-range hopping that turns into an Arrhenius activation as the transition is approached. With further decrease in static disorder, superconductivity sets in and the transition temperature increases towards a value of ≈ 3.3 K. The transition between a superconducting phase and an insulating one is also accompanied by a sign and anisotropy change in the magnetoresistance of the films. These results are discussed in light of recent theories.

I. INTRODUCTION

The disorder-induced metal-insulator transition (MIT) has been a subject of intense research for many years.¹ Renewed interest in this zero-temperature phase transition followed the scaling approach to the problem by Thouless² and Abrahams *et al.*³ These theories gave fresh insights and new predictions, many of which were experimentally confirmed during the last decade. The scaling picture describes the MIT as being a continuous process characterized by a correlation length ξ_L that diverges at the transition

$$\xi_L = \xi_0(1 - g_0/g_C)^{-\nu}, \quad (1)$$

where ξ_0 is the microscopic length, g_0 is a dimensionless conductance evaluated at the microscopic length, g_C is the critical conductance for the system under study, and ν is a critical exponent believed to be of order unity.¹ The transition reflects the fact that electronic wave functions become spatially localized, with a typical localization length, ξ_L . As the static disorder increases, states below the mobility edge, E_C , become localized and the system turns insulating at absolute zero when $E_C \geq E_F$.

The influence of electron-electron interactions on the above picture is less well understood. Coulomb correlations are expected to be important near the MIT and several authors have predicted some qualitative modifications to the nature of the transition due to them.⁴

Another, possibly related, issue is the disorder-induced transition in a system where the ground state of the metallic phase is superconducting. This may be interesting for two reasons. The pairing mechanism that causes k -space ordering in the superconducting phase may lead to real-space pairing in the insulating state characterized by a gap in the single-particle density of states.⁵ This can be brought about by a sufficiently strong electron-phonon interaction overcoming the Coulomb on-site repulsion which, therefore, makes double occupation of levels energetically favorable. Near the MIT, where ξ_L is large, such a scenario is quite feasible.

The other aspect of this problem is the possible coexistence of superconducting and insulating behavior. Namely, could a superconducting ground state be formed

from localized wave functions. The theoretical aspects of this question have been addressed in a number of papers.⁶ Despite the different approaches taken by different researchers, the predictions were essentially the same. Coexistence of superconducting and insulating phases is expected if the following two conditions are met:

$$\xi_L > \xi_S, \quad (2a)$$

$$\Delta_L < \Delta_S, \quad (2b)$$

where ξ_S and Δ_S are the superconducting coherence length and pair potential, respectively, and $\Delta_L = 1/N(0)\xi_L^3$ is the typical energy separation between localized sites. [$N(0)$ is the density of states at the Fermi level.] The physical plausibility of these conditions is transparent. It is easy to see that condition (2b) is very stringent given the smallness of Δ_S (typically few degrees K) in comparison with the natural scale of the energy separation between levels in the insulating phase (being essentially set by E_F once $\xi_L \rightarrow \xi_0$). This, in turn, places a severe requirement on sample uniformity needed for the experimental^{7,8} observation of the coexistence.

A different theoretical approach⁹ was motivated by experiments done on ultrathin superconducting films where the effective disorder was controlled by changing the film thickness.⁸ In this approach, a direct superconductor to insulator transition (SIT) is described as a process where the disorder drives a Bose-condensed superfluid into an insulating, "glassy," state where the Bose particles are localized. These theories are based on scaling-type arguments and do not explicitly address the conditions for the observation of such a transition.

In this paper we report on a low-temperature study performed on amorphous indium-oxide samples where the static disorder could be varied over a wide range. Our main purpose in this work is to study the systematics of the SIT in a three-dimensional system where (in contrast with the two-dimensional case) a metal-insulator transition should occur.

Section II describes sample preparation and characterization techniques used in the study as well as the measurement methods. Section III includes our experimental

results. The data analysis and their implications are discussed in Sec. IV.

II. EXPERIMENT

In this section we will describe some of the experimental procedures employed in this work. A more detailed account is given in Ref. 10. Here we merely emphasize details that are of special significance to the present work.

We have made extensive use of thermal annealing in this study to generate samples with different degrees of disorder from a given batch. The working routine for the low-temperature transport measurements was as follows: 2000-Å samples were prepared by *e*-gun evaporating high-purity (99.997%) In_2O_3 onto a SiO_2 substrate in a vacuum system maintaining a base pressure $< 10^{-6}$ Torr. The as-deposited film was mounted on the measurement probe and electrical leads were connected to it by soft soldering to indium contacts pressed onto the current and voltage probes. Six voltage probes on each sample enabled several different Hall and resistance measurements to be made in order to verify large-scale uniformity. The scatter in any two readings of the resistance on the same strip was less than 1%, while the scatter within a given evaporation batch never exceeded 5%. Typical room-temperature resistivities of the as-deposited films were in the 30–50 m Ω cm range and the carrier density, n (based on Hall effect measurements), was $2\text{--}5 \times 10^{21}$ cm $^{-3}$ throughout this study. Following the initial resistance and Hall effect measurements, the system was cooled down to liquid-helium temperatures where the low-temperature study was done. The system, with the sample still mounted, was then brought up to 40–60°C and the resistance as a function of time was monitored. It was typically observed that R goes down with time at a rate of up to 20% per hour dependent on R itself and on the temperature. The sample was then cooled back to room temperature where the same procedures for uniformity tests and determination of sample parameters mentioned above were repeated. As long as this thermal annealing was carried out in vacuum, the Hall voltage was found to be essentially independent of the value of R within a batch. We thus attribute the decrease in the resistance observed upon annealing to improved mobility.¹⁰

As a measure of the disorder in the samples we used the dimensionless parameter $k_F l$ estimated from the room-temperature resistivity and Hall effect measurements, using free-electron expressions.¹¹ This parameter is clearly monotonic with disorder, is experimentally well defined, and is still descriptive of the static disorder even when its value is smaller than unity (and then neither k_F nor l are “good” parameters). The important caveat that should be borne in mind in this regard is that when $k_F l < 1$, l must not be interpreted as a “semiclassical” mean free path.

A major concern in such studies is the quality of the samples from the point of view of uniformity and homogeneity. We have made films with dimensions as small as 50 μm and as big as 2 cm which showed the same sheet resistance (to within 1%) when simultaneously prepared

or annealed. This observation should only be taken as evidence for large-scale homogeneity. On small enough scales, we expect our films, and for that matter, all disordered conductors, to be *inherently* inhomogeneous by their very nature.

In order to gain more insight for the microstructure and for physical changes accompanying the decrease of the resistance due to thermal annealing, we have studied the structural aspects of our films by electron microscopy performed on films deposited with the same nominal conditions as described above onto carbon-coated Cu grids. (Test measurements were done using SiO_2 substrates with similar results.) Figure 1 illustrates a typical micrograph and an associated diffraction pattern. We have also studied films much thinner than that shown in this figure and a few with thicknesses of 1000–2000 Å. The following facts were discovered: Physical continuity (area coverage greater than 80–90%) is attained for films with nominal thicknesses as small as 15–20 Å. The “clumpiness,” clearly observed in the micrograph of the 500-Å film (Fig. 1) is presumably an inherent property of the films, as it changes little from 30 to 500 Å (six different thicknesses in this range were looked at). This clumpiness, which has a scale of ≈ 20 Å, becomes less apparent for films that are thicker than ≈ 1000 Å, giving the impression of a more uniform structure. The likely interpretation of this latter fact is that it is the decrease in contrast in the imaging process due to the increase of inelastic scattering that is observed for the thicker films rather than a real difference in clumpiness. Judging from the diffraction patterns, the material is always amorphous and we never observed inclusions of a crystalline component in the as-prepared films nor in films heat treated at temperatures below 130°C. We have also never observed evidence for “free” indium in any of the samples studied. We can therefore rule out the possibility that the observed SIT is a simple indium percolation transition. Within the resolution of the microscope, we were not able to observe any change in the structure of the films even for samples where



FIG. 1. Diffraction pattern and electron micrograph of a 500-Å sample prepared in the same way as the samples used for the transport study.

thermal annealing caused an order of magnitude change in the resistivity.

All electrical measurements reported below were carried out by a standard four-probe dc technique employing a Keithley 220 current source and a Keithley 196 digital voltmeter or a Keithley 617 electrometer. Temperature was measured using a calibrated Ge thermometer or a Pt resistor (for $T \geq 10$ K). The electronic instruments were connected via IEEE to a PC that controlled data acquisition. Low-temperature measurements were done in an immersion-type pumped-helium cryostat mounted in the gap of a split-coil electromagnet. The cryostat was rotatable up to 180° , thus allowing measurements as a function of the angle between the field direction and the sample plane.

III. RESULTS

Figure 2 depicts the resistance versus temperature, $R(T)$, for one of the studied batches, illustrating the evolution of the low-temperature behavior as a function of static disorder. The initial $R(T)$ in this series follows an Arrhenius-type behavior, namely, $R(T) = R_0 \exp(T_0/T)$. After thermal annealing, both R_0 and T_0 decrease and eventually a maximum in $R(T)$ is observed which presumably indicates the occurrence of superconductivity at lower temperatures. For samples with still higher values of $k_F l$ this scenario can be directly confirmed. A typical case is depicted in Fig. 3. The resistance of the sample drops fairly sharply (2 orders of magnitude per

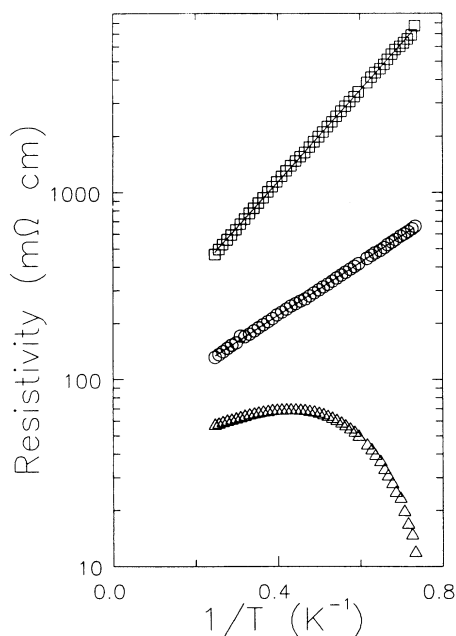


FIG. 2. Resistivity vs temperature of a typical batch of indium-oxide samples measured between 1.3 and 4.11 K. The upper curve is for the as-deposited film. The lower curves depict the $R(T)$ of the same sample after thermal annealing. The solid lines for the top two curves are fits to an Arrhenius behavior from which the various T_0 values were extracted. $k_F l$ values of these samples are 0.177 (\square), 0.21 (\circ), and 0.272 (\triangle). The sample thickness is 2000 Å and $n = 4 \times 10^{21}$.

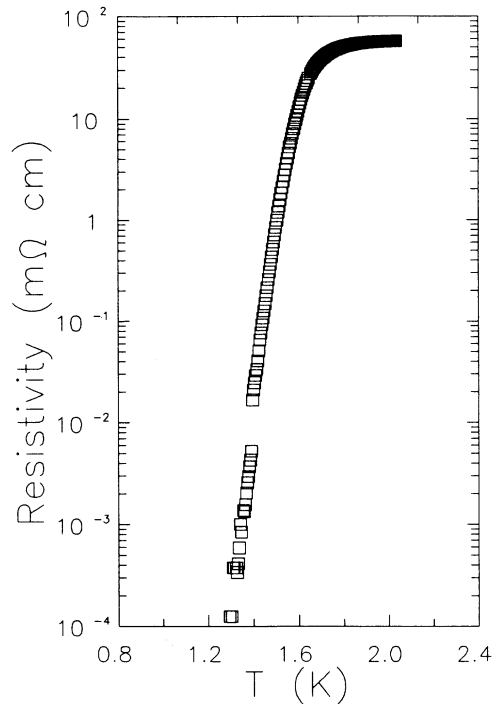


FIG. 3. Resistivity vs temperature for a sample with $k_F l = 0.325$. Note the different abscissa.

0.1 K) below a characteristic T_c . This temperature, defined as the temperature where the resistivity drops to 50% of its normal-state value, increases monotonically with $k_F l$ up to $T \approx 3.3$ K for the most “metallic” sample. It is noted that the tail of the $R(T)$ curve is smooth and there is no indication for a “shoulder” or any other hint of “reentrance behavior” which might have suggested gross inhomogeneity in the films.⁸

The general aspects of the SIT are summarized in Fig. 4. Two different symbols are used to designate either T_0 for samples that are insulating or T_c , for samples that exhibit superconductivity (at $T \geq 1.3$ K). Both characteristic energies are plotted as a function of the static disorder as a common abscissa. In a rather narrow range of $k_F l \approx 0.25$ – 0.3 the system turns from “insulating” to “superconducting.”

We follow Fiory and Hebard¹² and fit the superconducting data points using $T_c = T_{c0} \{1 - [(k_F l)^c / (k_F l)]^2\}$, which results in $(k_F l)^c \approx 0.2$ and $T_{c0} \approx 3.3$ K. We are well aware of the limitations of that expression (valid only in the $k_F l \gg 1$ range) and therefore merely regard it as a guide to the eye. For the insulating data points we use Eq. (1) with $k_F l$ replacing g as the disorder parameter and taking $\nu = 1$, resulting in $(k_F l)^c = 0.35 \pm 0.03$. The implications of the fact that the two plots intersect at a finite temperature (of the order of 2 K) and that the two values thus obtained for $(k_F l)^c$ significantly differ will be discussed in Sec. IV.

Yet another value for the “critical” $k_F l$ can be obtained from the magnetoresistance data of these samples. In Figs. 5(a) and 5(b) we present the temperature dependence of the resistance and the magnetoresistance, re-

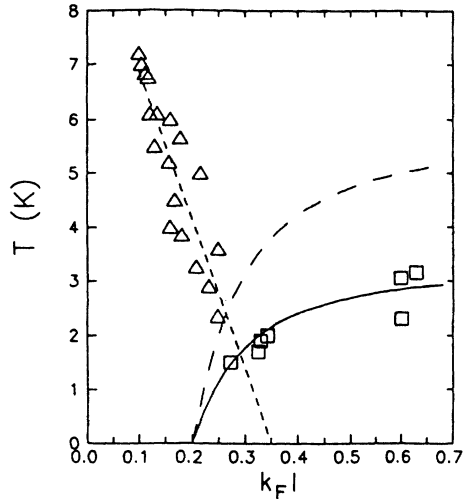


FIG. 4. The dependence of the pertinent energies, T_0 (Δ) (for insulating samples) and T_c (\square) (for superconducting samples) on disorder ($k_F l$). The solid line is a fit to the superconducting data points (see Sec. III) while the long-dashed curve fits the same data using $\Delta_S = 1.76 T_c$ following the BCS expression. The short-dashed line best fits the insulating data points (see text) with $(k_F l)^c = 0.35 \pm 0.03$.

spectively, for one batch of “insulating” films. In terms of the $R(T)$ data [Fig. 5(a)] even the least disordered sample in the batch exhibits activated behavior with only a small deviation at the lowest temperatures. However, the magnetoresistance as a function of temperature [Fig. 5(b)] clearly separates the samples into two distinct groups: The three more resistive samples show purely negative magnetoresistance which is weakly temperature dependent, essentially independent of disorder and isotropic (i.e., independent of the field orientation). By contrast, the magnetoresistance of the least disordered sample is purely positive, strongly temperature dependent, and anisotropic (in the parallel field orientation the fractional change of the resistance was about one-half to one-third of the respective value in a perpendicular field). This presumably indicates that in the latter sample there are significant superconductive fluctuations which grow bigger as the temperature is lowered and possibly the system will become truly superconducting at sufficiently low temperatures. The behavior depicted in Figs. 5(a) and 5(b) was reproduced on two other batches with similar values of $k_F l$. Bearing in mind the relative sharpness of the transition, this reproducibility is a strong indication of a fairly high degree of homogeneity. If the qualitative features of the magnetoresistance are taken as the criteria for the transition, the “critical $k_F l$ ” is ≈ 0.2 , in support of the value obtained from the extrapolation of the superconducting data points.

Finally, for sufficiently strong disorder ($k_F l < 0.1$), the $R(T)$ of the samples takes on the familiar Mott variable range hopping law: $R(T) = R_0 \exp[(T_*/T)^{1/4}]$ in the same temperature range. A typical case is illustrated in Fig. 6. Following thermal annealing, the $R(T)$ of such a sample turned into simple activation with a T_0 that was consistent with its $k_F l$.

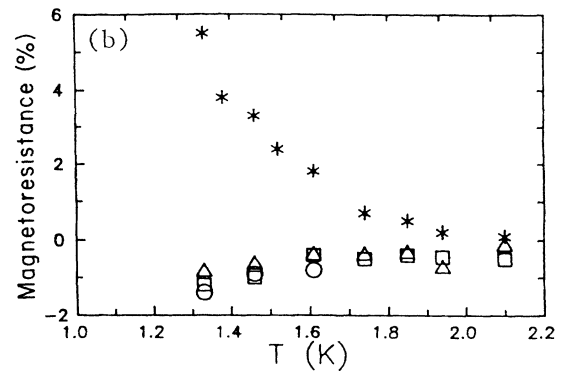
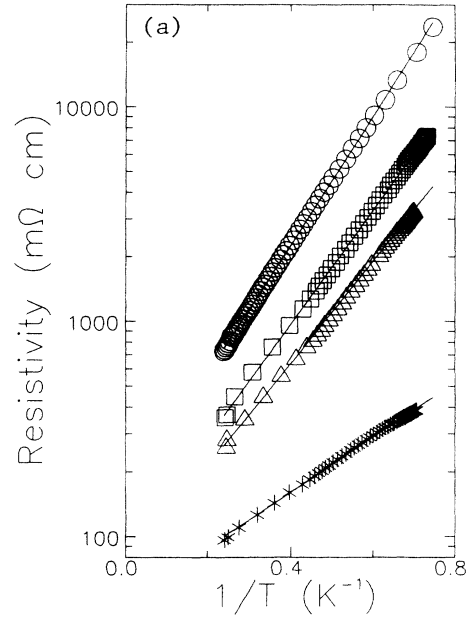


FIG. 5. (a) Resistivity and (b) magnetoresistance at 7 kOe as a function of temperature for four different stages of anneal produced by heat treating a single film as described in the text. The $k_F l$ values for these samples are 0.1 (\circ), 0.12 (\square), 0.129 (Δ), 0.231 ($*$). The magnetoresistance data presented here were taken with the field perpendicular to the plane of the film.

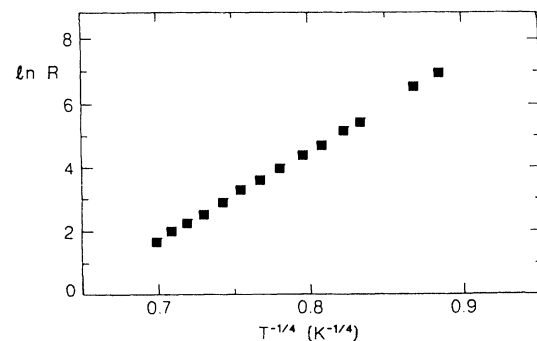


FIG. 6. Resistance as a function of temperature for a highly disordered sample ($k_F l = 0.04$) exhibiting Mott's VRH, with $T_* = 6 \times 10^5$ K. R is measured in $M\Omega$. Sample thickness is 2000 Å and approximately one square was measured.

IV. ANALYSIS AND DISCUSSION

The fact that the extrapolated curves in Fig. 4 cross at a finite temperature [resulting in two different estimates for $(k_F l)^c$] suggests a region of superconducting and insulating coexistence not unlike the one conceived by the single-particle theories of Ref. 6. The main point we wish to make in this section is that despite this qualitative agreement, the coexistence region observed is *not* due to the simultaneous fulfillment of conditions (2a) and (2b). To show this, we have calculated, for each of the samples, ξ_L , ξ_S , Δ_L , and Δ_S , which can be cross compared with regard to conditions (2a) and (2b) in Figs. 7(a) and 7(b),

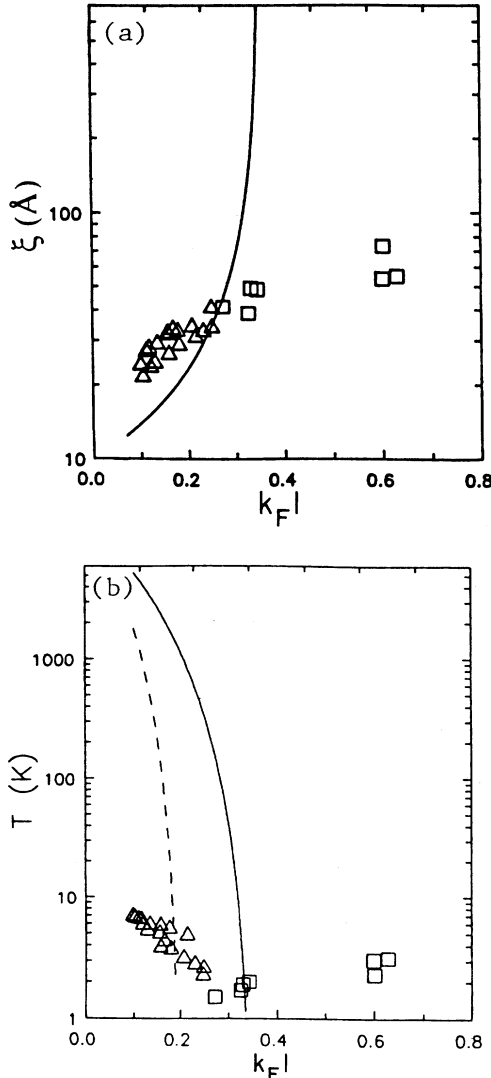


FIG. 7. (a) The relevant correlation lengths as a function of $k_F l$. The solid curve is a plot of ξ_L according to the scaling expression with $k_F l^c = 0.35$. The symbols stand for calculated values of ξ_S for each of the samples in Fig. 4 (see text). Squares and triangles are used to designate superconducting and insulating films, respectively. (b) Same as in Fig. 4, with an additional energy scale plotted: The solid curve is a plot of Δ_L using $k_F l^c = 0.35$, while the dashed curve uses $k_F l^c = 0.2$. Note the logarithmic ordinate.

respectively. These parameters were determined as follows. ξ_L was calculated by the scaling relation [Eq. (1)], replacing g with $k_F l$ as the disorder parameter and using $\xi_0 = 10 \text{ \AA}$, $\nu = 1$ and $(k_F l)^c \approx 0.35$, which was estimated as described in the previous section. Δ_L was then determined through $\Delta_L = 1/N(0)\xi_L^3$. [$N(0)$ was inferred from the carrier density using free-electron expressions.] ξ_S was estimated from the Ginzburg-Landau expression $\xi_S = (\xi l)^{1/2}$, where ξ is the bulk value of the superconducting coherence length.¹³ Finally, Δ_S was set by the measured T_c using the BCS expression $\Delta_S = 1.76T_c$. As can be seen in Figs. 7(a) and 7(b), condition (2a) is reasonably well obeyed while condition (2b) is violated in the sense that 3–4 samples exhibit superconductivity despite their Δ_L being bigger than Δ_S . It may appear that this problem can be avoided by shifting $(k_F l)^c$ to lower values. However, this can only account for the superconducting samples. The discrepancy between the two characteristic energies (i.e., $k_B T_0$ and Δ_L) for the dozen or so insulating samples, which is about 3 orders of magnitude, is too large to be reconciled by refitting the data [cf. Fig. 7(b)]. For instance, if one tries to force $(k_F l)^c$ to be ≈ 0.2 (which is already hard to justify on the basis of the data shown), the resulting Δ_L still exceeds $k_B T_0$ by two orders of magnitude. To bridge this difference it is necessary to assume that ξ_0 is much larger than 10 \AA . We specifically rule out such a possibility since ξ_0 should not be much larger than $n^{-1/3}$ ($\approx 7 \text{ \AA}$ in our samples). To further check on this important point we analyzed the $R(T)$ of a highly disordered sample (cf. Fig. 6). This sample is far enough from the transition and therefore its ξ_L should be close to ξ_0 . Using Mott's formula, $k_B T_* = [N(0)\xi_L^3]^{-1}$, with T_* from the logarithmic slope and the estimate $N(0)$ for this particular sample, one gets $\xi_L \approx 10 \text{ \AA}$, which compares very favorably with the inter-carrier distance and with our estimates for ξ_0 .

Another way to see the quantitative discrepancy between theory⁶ and experiment is to note that the width of the transition region observed in Fig. 4 appears to be larger than expected. The range of "overlap" in the curves is of the order of 0.3 in relative units. Coexistence in the sense conceived by the theories is limited to a much narrower region⁶ of relative width Δ_S/E_F ($\approx 10^{-3}$ in our system).

This discrepancy between the single-particle theories and our experiment may be to some degree due to artifacts such as spatial inhomogeneities. As mentioned in Sec. II, disordered films are inhomogeneous by nature. It is not clear that long-range potential fluctuations,¹⁴ for instance, may be neglected. The usual argument for disregarding such complications relies on the theoretical observation that at $T \rightarrow 0$ classical percolation should not be important and quantum effects will be dominant. The present case, however, involves a natural cutoff (T_c) which may not be low enough to justify the former argument. We regard this as an open question.

The effects of many-body interactions on the SIT have been considered by some recent theories.^{9,15} These theories, however, do not specify the microscopic mechanism that underlies the transition. This makes it hard to

get even a qualitative prediction on the behavior of, e.g., the magnetoresistance near the transition, for which we have quite specific experimental data. More importantly, it seems to us that the question of the transport mechanism in the insulating side near the SIT, which those theories do not address, is of paramount importance. Obviously, a key feature in the observed transition is the interplay between the condensation energy of the superconducting state (T_c) and a characteristic energy of the insulating phase (T_0): The transition from a superconductor to an insulator is observed to occur at, or close to, the point where the two are equal (Fig. 4). It is then reasonable to expect that it is $k_B T_0$, rather than Δ_L , that plays the role of the relevant energy in this problem. This makes it imperative to understand the physical origin of the Arrhenius law of the $R(T)$ for the just-insulating samples. In particular, one needs to know what determines the characteristic energy $k_B T_0$. There are several mechanisms that are known to lead to an Arrhenius activation near the MIT. However, only nearest-neighbor hopping¹⁶ and excitation to the mobility edge¹⁷ are detailed enough to be critically compared with our experimental results. Both can be shown to be inapplicable to the present case using essentially the same arguments as raised above in connection with the failure of conditions (2a) and (2b). Further progress in this problem must

await the full elucidation of this mechanism.

In summary, we have presented a comprehensive experimental study of the SIT in a three-dimensional amorphous metal. A detailed analysis of our data using a single-particle approach to the SIT leads to some important quantitative discrepancies. This may suggest the necessity to treat this problem from a many-body point of view. This is hardly surprising: Many-body effects are manifestly dominant on the superconducting side of the transition and it is natural to expect that their presence will modify the physics underlying both the transition and the insulating phase adjacent to it. Current theories of the SIT have adopted this point of view but are still not detailed enough to describe the specific behavior near the transition. It is hoped that our results will encourage further theoretical developments on this important problem.

ACKNOWLEDGMENTS

The authors gratefully acknowledge illuminating discussions with P. W. Anderson, W. I. Glaberson, G. Deutscher, Y. Imry, M. P. A. Fisher, A. Frydman, M. Pollak, M. Strongin, D. J. Thouless, and M. Weger. This research has been supported by a grant administered by the Israel-US Binational Science Foundation.

*Present address: Department of Physics, Princeton University, Princeton, NJ 08544.

¹P. A. Lee and T. V. Ramakrishnan, *Rev. Mod. Phys.* **57**, 287 (1985).

²D. J. Thouless, *Phys. Rev. Lett.* **39**, 1167 (1977).

³E. Abrahams, P. W. Anderson, D. C. Licciardello, and T. V. Ramakrishnan, *Phys. Rev. Lett.* **43**, 718 (1979).

⁴A. M. Finkelshtein, *Z. Phys. B* **56**, 189 (1984); P. A. Lee and T. V. Ramakrishnan, *Rev. Mod. Phys.* **57**, 287 (1985).

⁵P. W. Anderson, *Phys. Rev. Lett.* **34**, 953 (1975).

⁶L. N. Bulaevskii and M. V. Sadvovskii, *J. Low Temp. Phys.* **59**, 89 (1985); A. Kapitulnik and G. Kotliar, *Phys. Rev. Lett.* **54**, 473 (1985); G. Kotliar and A. Kapitulnik, *Phys. Rev. B* **33**, 3146 (1986); M. Ma and P. A. Lee, *ibid.* **22**, 5658 (1985).

⁷M. Strongin, R. S. Thompson, O. F. Kammerer, and J. E. Crow, *Phys. Rev. B* **2**, 1078 (1970); Y. Imry and M. Strongin, *ibid.* **24**, 6353 (1981); Y. Shapira and G. Deutscher, *ibid.* **27**, 4463 (1983).

⁸H. M. Jaeger, D. B. Haviland, B. G. Orr, and A. M. Goldman, *Phys. Rev. B* **40**, 182 (1989); D. B. Haviland, Y. Liu, and A.

M. Goldman, *Phys. Rev. Lett.* **62**, 2180 (1989), and references therein.

⁹M. P. A. Fisher, G. Grinstein, and S. M. Girvin, *Phys. Rev. Lett.* **64**, 587 (1990); M. P. A. Fisher, P. B. Weichman, G. Grinstein, and D. S. Fisher, *Phys. Rev. B* **40**, 546 (1989).

¹⁰Z. Ovadyahu, *J. Phys. C* **19**, 5187 (1986).

¹¹G. Bergmann, *Phys. Rep.* **27**, 159 (1976).

¹²A. T. Fiory and A. F. Hebard, *Phys. Rev. Lett.* **52**, 2057 (1984).

¹³Several authors (Ref. 6 above) have suggested the use of $\xi_S = (\xi l^2)^{1/3}$ rather than $\xi_S = (\xi l)^{1/2}$ in the critical region near the MIT. This modification, important in principle, is not essential to the interpretation of our data.

¹⁴M. Pollak, *Phys. Status Solidi B* **66**, 483 (1974).

¹⁵M. Kaveh and N. F. Mott, *Phys. Rev. Lett.* **68**, 1904 (1992).

¹⁶B. I. Shklovskii and A. L. Efros, *Electronic Properties of Doped Semiconductors* (Springer-Verlag, Berlin, 1984).

¹⁷N. F. Mott and G. A. Davis, *Electronic Processes in Non-Crystalline Materials*, 2nd ed. (Clarendon, Oxford, 1979).

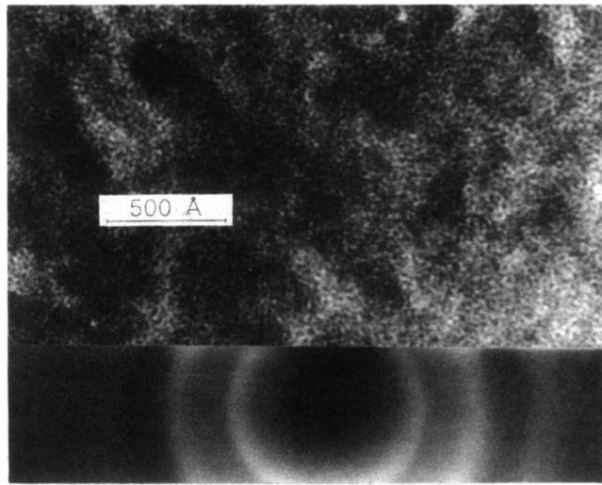


FIG. 1. Diffraction pattern and electron micrograph of a 500-Å sample prepared in the same way as the samples used for the transport study.